Retinoic acid deficiency mediated by temporospatial loss of *Rdh10* underlies the etiology of midfacial defects

Yanran Wu

Department of Orthodontics and Dentofacial Orthopedics,

Graduate School of Dentistry, Osaka University

Abstract

Embryonic craniofacial development depends on the outgrowth and fusion of multiple facial primordia which are populated with cranial neural crest cells and covered by the facial ectoderm. Any disturbance in the developmental processes or tissues could result in a range of craniofacial deformities, including midfacial cleft. In humans, midfacial cleft, a subtype of orofacial cleft, is identified as a vertical cleft through the center of the lip and occurs rarely compared to the most common unilateral or bilateral cleft lip and/or palate. In the present study, we showed that inactivation of *Rdh10* by tamoxifen treatment at E7.0 resulted in substantial reduction of retinoic acid (RA) signaling in the developing frontonasal process and a variety of midfacial defects, including midfacial cleft, agenesis of upper incisors, and ectopic nodules with chondrogenesis. Elevated apoptosis in migrated cranial neural crest cells and substantial reduction of *Alx1* and *Alx3* transcription in the developing frontonasal process are suggested to underlie the etiology of midfacial cleft in *Rdh10*-deficient mice. Furthermore, persistent *Shh* signaling in the ventral forebrain, as well as partial abrogation of midfacial defects by inhibition of *Hh* signaling, in the Rdh10 mutant indicate that misregulation of S*hh* signaling due to reduced RA signaling underlies the etiology of midfacial defects. Together, these data indicate that the spatiotemporal distribution of *Rdh10* and RA signaling during early embryonic craniofacial development is important for orchestrating molecules which govern midfacial development.

Introduction

Embryonic craniofacial development relies on the outgrowth and fusion of five facial primordia: the frontonasal process, two pairs of maxillary processes and mandibular processes. These primordia are populated by cranial neural crest cells and covered by the facial ectoderm. Any disturbance in these developmental processes or tissues could result in a range of craniofacial deformities, including midfacial cleft. The incidence of midfacial cleft, which is a subtype of orofacial cleft, is low compared to the common unilateral or bilateral cleft lip and/or palate, and thus the mechanisms remain largely elusive (Apesos and Anigian 1993; Mishra et al. 2015).

Retinoic acid (RA), an active derivative of Vitamin A, is a diffusible molecule, and RA signaling is critical for embryonic craniofacial development (Metzler and Sandell 2016). It has been suggested that either excess or deficiency of RA signaling could lead to teratogenic effects, including orofacial cleft (Shannon et al. 2017). Especially, deficiency of embryonic RA signaling due to loss of *Rdh10*, the gene that encodes the metabolic enzyme for synthesizing RA, has been shown to cause midfacial cleft (Sandell et al. 2007). However, the detailed cellular and molecular mechanisms that produce this midfacial cleft are not fully understood.

For these reasons, we utilized tamoxifen-induced *Rdh10* knock-out mice for investigating the cellular and molecular mechanisms of midfacial cleft caused by RA deficiency. We discovered that eliminating *Rdh10* expression at E7.0 resulted in substantial reduction of RA signaling, especially in the developing frontonasal process, and a variety of midfacial defects, including midfacial cleft, agenesis of upper incisors, and ectopic nodules with

chondrogenesis in the medial nasal region. Significant elevation of apoptosis in migrated cranial neural crest cells, which was caused by downregulation of aristaless-like (*Alx*) family genes, was shown to underlie the etiology of midfacial cleft. Exaggerated sonic hedgehog (*Shh)* signaling also contributed to the midfacial cleft phenotype, which could be blocked by administering cyclopamine, an inhibitor of hedgehog (*Hh)* signaling. Elevated fibroblast growth factor 8 (*Fgf8)* and *Wnt* signaling seem to underlie the ectopic cartilage formation in the frontonasal process. Additionally, upper incisor development was disturbed by impaired proliferation and invagination of dental lamina. Altogether, our findings have uncovered a novel signaling pathway and cellular behavior which underpin the etiology of multiple midfacial defects.

Materials and Methods

Mice, Tamoxifen Administration and Cyclopamine Injection

Cre-ERT2:RDH10^{flox} and *RARE-lacZ* mice were used and maintained as previously described (Kurosaka et al. 2017; Sandell et al. 2007). In order to eliminate RDH10 from developing embryos, *Rdh10*$^{flox/flox}$ female mice were crossed with *Cre-ERT2:Rdh10*$^{flox/flox}$ male mice followed by stage-specific tamoxifen administration. We administered 5 mg of tamoxifen (Sigma-Aldrich, #T5648) and 1 mg of progesterone (Sigma, #P3972) in 200 µl of corn oil (Sigma-Aldrich, #C8267) to individual pregnant dams via oral gavage at either E7.0 or E7.5. The morning of detecting the vaginal plug was defined as E0.5. Cyclopamine (LKT, #c9710) was administered to pregnant dams at a dosage of 20 mg/kg body weight via intraperitoneal injection at E11.0 after tamoxifen treatment at E7.0. Cyclopamine was

suspended at 1 mg/ml in a 45% w/v solution of (2-Hydroxypropyl)-β-cyclodextrin solution (Sigma, #H5784) (Firulli et al. 2014).

All animal experiments were performed in accordance with the guidelines of the Animal Care and Use Committee of the Osaka University Graduate School of Dentistry, Osaka, Japan. The Committee on the Ethics of Animal Experiments of the same university approved the study protocol (permit number: 動歯 26-020-0 and 遺 04506). Unless otherwise indicated, we used a minimum of 3 embryos from multiple distinct litters for each parameter analyzed in this study.

Immunohistochemistry and TUNEL Staining

Whole-mount nuclear fluorescent imaging (Sandell et al. 2012a) was utilized to capture embryonic morphological features. The embryos were fixed in 4% PFA and incubated overnight in 1:1000 DAPI dilution at 4℃ (Dojindo, #D523-10). Immunostaining of frozen sections was performed as previously described (Kurosaka et al. 2017). Antibodies against phospho-HISTONE-H3 (#05806, 1:200, Millipore), E-CADHERIN (#3195, 1:200, Cell Signaling Technology), β-CATENIN (PY489-B-CATENIN #10144551, 1:50, DSHB), and SOX2 (#97959, 1:100, Abcam) were used with appropriate secondary antibodies for detecting each protein's localization. Apoptotic cells were detected by using an in situ cell death detection kit (Roche, #11684795910) following the manufacturer´s instructions.

Whole-mount *In Situ* Hybridization

Whole-mount *in situ* hybridization was performed as described previously (Kurosaka et al. 2014). The digoxigenin-labelled antisense RNA probes were produced using a DIG RNA labeling kit (Roche, #11277073910) according to the manufacturer's protocol. A minimum of three embryos of each sample were examined per probe.

***β-galactosidase* Staining of *RARE-lacZ* Reporter Mice**

Staining for *β-galactosidase* expression in *RARE-lacZ* reporter mice was performed by fixing the tissue in 2% formaldehyde and 0.8% glutaraldehyde solution for 30 min at 4℃ followed by treatment with 1mg/ml X-gal (Promega, #V3941) solution for 2 hours at room temperature.

Histological Analysis

E13.5 and E16.5 embryos were fixed in 4% PFA overnight. Paraffin embedding and preparation of 7-μm-thick histological sections followed by hematoxylin and eosin staining were performed according to standard histological protocols.

Statistical Analysis

Statistical significance in Figure 2, 4 and 5 was assessed using Student´s *t*-test. *P* values of less than 0.05 were defined as significant in all experiments.

Results

Loss of *Rdh10* and RA Signaling in Developing Frontonasal Process Leads to Various Midfacial Defects in Mice

To compare the spatiotemporal distribution of *Rdh10*-mediated RA signaling between wild-type and *CreERT2: Rdh10*$^{flox/flox}$ mice during the developmental stage of frontonasal process, *RARE-lacZ* expression was detected by β-galactosidase staining (Rossant et al. 1991). Following tamoxifen treatment at E7.0, substantial reduction of *RARE-lacZ* expression was detected in the *CreERT2: Rdh10*$^{flox/flox}$ frontonasal process at E9.5 (Fig. 1A, D) and E10.5 (Fig. 1B, E). At the same time, whole-mount *in situ* hybridization of *Rdh10* showed a noticeable reduction in the *CreERT2: Rdh10*$^{flox/flox}$ frontonasal process (Fig. 1C, F). These data indicate that *Rdh10* expression at around E7.0 plays a dominant function in activating RA signaling in the developing frontonasal process.

Previous studies have reported multiple craniofacial phenotypes of *Rdh10* mutants (Friedl et al. 2019; Kurosaka et al. 2017; Metzler et al. 2018; Sandell et al. 2007). In the present study, we administered tamoxifen at either E7.0 or E7.5, and we found that 36 of 38 (92.6%) *CreERT2: Rdh10*$^{flox/flox}$ embryos treated with tamoxifen at E7.0 showed midfacial cleft (referred as complete midline facial cleft). In contrast, 11 of 53 (20.8%) *CreERT2: Rdh10*$^{flox/flox}$ embryos treated with tamoxifen at E7.5 showed midfacial cleft. Nuclear

fluorescent imaging was utilized to compare the craniofacial morphology between wild-type and *CreERT2: Rdh10*$^{flox/flox}$ embryos treated with tamoxifen at E7.0. In embryos at E10.5 (n=11), there was no noticeable morphological difference (Fig. 1G, J), whereas in embryos at E11.5 (n=14), medial nasal processes failed to fuse in the midline of the face in *CreERT2: Rdh10*$^{flox/flox}$ mice in contrast to wild-type mice (Fig. 1H, K). In embryos at E12.5 (n=11), midfacial cleft became prominent and ectopic nodules formed in the medial nasal region of *CreERT2: Rdh10*$^{flox/flox}$ mice relative to wild-type mice (Fig. 1I, L).

Frontal histological sections of E16.5 heads showed abnormal mesenchymal condensation and rod-like chondrogenesis on the face where the ectopic nodules formed in *CreERT2: Rdh10*$^{flox/flox}$ mice (n=4) (Fig. 1 P). We also detected a variety of upper incisor defects in histological sections. Missing upper incisors were frequently concurrent with midfacial cleft in these *CreERT2: Rdh10*$^{flox/flox}$ mutants (n=19/21) (Fig. 1Q). The majority of *CreERT2: Rdh10*$^{flox/flox}$ mice without midfacial cleft exhibited split upper incisors (n=4/7) (Fig. 1R). In addition, the upper incisors that existed in *CreERT2: Rdh10*$^{flox/flox}$ mutants were smaller in size (Fig. 1Q, R). In contrast, upper molars did not show noticeable deformities at E16.5 (Appendix figure. 1). These results indicate that the severity of midfacial defects is correlated with the time point of *Rdh10* elimination. Additionally, the craniofacial defects in *CreERT2: Rdh10*$^{flox/flox}$ mice exhibit severer phenotypes in the derivatives of the frontonasal process than in those of the maxillary process.

***Rdh10*-Mediated RA Signaling Is Required for the Survival of Migrated Cranial Neural Crest Cells by Maintaining Expression of *Alx* Family Genes**

The frontonasal process is populated by cranial neural crest cells, and its disturbance could result in multiple craniofacial defects, including midfacial cleft. In order to investigate the development of cranial neural crest cells, *in situ* hybridization of *Tfap2a* and *Sox9* was performed at E9.5. The expression patterns of both genes exhibited no noticeable difference in the frontonasal process between wild-type and *CreERT2: Rdh10*$^{flox/flox}$ mice (Fig. 2A, B, F and G). These results indicate that the formation and migration of cranial neural crest cells are not severely influenced by reduced RA signaling. To further assess the behavior of post-migratory cranial neural crest cells, TUNEL staining and immunostaining of phospho-Histone-H3 (PHH3) were used to detect apoptosis and cell proliferation in the E10.5 frontonasal process. We detected significant elevation of apoptosis in the frontonasal mesenchyme of E10.5 *CreERT2: Rdh10*$^{flox/flox}$ embryos relative to wild-type (Fig. 2C, E and H). The number of PHH3-positive cells in the frontonasal mesenchyme did not show a significant difference between wild-type and *CreERT2: Rdh10*$^{flox/flox}$ mice (Fig. 2D, I and J). These data indicate that proper RA signaling is required for the survival of post-migratory cranial neural crest cells, and elevated apoptosis in the frontonasal mesenchyme underlies the cellular etiology of midfacial cleft.

In order to investigate possible molecular mechanisms which underlie the craniofacial defects in *CreERT2: Rdh10*$^{flox/flox}$ mice, we evaluated the result of RNAseq (Kurosaka et al. 2017) and selected several genes which showed significant differences and were known to be critical for midfacial development. Consistently, we detected reduced expression of *Alx1* and *Alx3* (Fig. 2K, L, O and P), of which mutations are associated with midfacial cleft accompanied by elevated apoptosis in the frontonasal process of mice (Beverdam et al. 2001). We also detected elevated expression of *Fgf8* and β-CATENIN in the ectoderm of

the medial nasal process of E10.5 *CreERT2: Rdh10*$^{flox/flox}$ mice compared to wild-type (Fig. 2M, N, Q and R). These results indicate interactions between RA signaling and other signaling molecules which are critical for midfacial development.

Disturbed Expression of *Shh* by Reduced RA Signaling Contributes to Midfacial Defects

Shh signaling is one of the most well-known signaling pathways which play crucial roles for midfacial development (Abzhanov and Tabin 2004; Brugmann et al. 2010). Our recent study also showed a critical interaction of RA and *Shh* signaling during craniofacial development (Wang et al. 2019). For these reasons, we compared the differences of *Shh* signaling between wild-type and *CreERT2: Rdh10*$^{flox/flox}$ embryos (n=5 embryos each). We found reduced expression of *Shh* in *CreERT2: Rdh10*$^{flox/flox}$ dental epithelium at E10.5 and E11.5 (Fig. 3A, B, E and F). Conversely, we detected persistent expansion of *Shh* in *CreERT2: Rdh10*$^{flox/flox}$ ventral forebrain starting at E11.5 (Fig. 3B, F). Moreover, *Ptch1* and *Gli1*, readout genes of *Shh* signaling, not only exhibited persistent expansion in the ventral forebrain but also ectopic expression in the midline of the face in E11.5 *CreERT2: Rdh10*$^{flox/flox}$ mice (Fig. 3C, D, G and H). These data indicate that reduced *Shh* expression in dental epithelium and persistent expansion of *Shh* signaling in the ventral forebrain caused by reduced RA underlie the etiology of detected midfacial defects.

Initiation of Upper Incisor Development Is Arrested by Reduced RA Signaling

In order to identify which developmental stage of incisor development is specifically influenced by reduced RA signaling, we assessed the expression of SOX2 and P21 to indicate dental lamina and dental placode (Sun et al. 2016; Thesleff 2003; Zhang et al. 2012). At E11.5, we detected lack of stratification and/or invagination with decreased cell proliferation in SOX2-expressing dental lamina of *CreERT2: Rdh10*$^{flox/flox}$ mice relative to wild-type (Fig. 4A, C, E and F) (n=3 embryos each). At E13.5, we also detected noticeable reduction of P21 expression in dental placode of *CreERT2: Rdh10*$^{flox/flox}$ mice (Fig. 4B, D) (n=3 embryos each). These results clearly indicate that upper incisor defects in *CreERT2: Rdh10*$^{flox/flox}$ mice begin at the initial stage.

We further analyzed dental mesenchyme and epithelium markers during the initiation of incisor development. *Pax9,* an early dental mesenchyme marker, showed substantial reduction in *CreERT2: Rdh10*$^{flox/flox}$ dental mesenchyme relative to wild-type at E10.5 (Fig. 4G, K) (n=4 embryos each). *Pitx2,* one of the earliest dental lamina markers, showed noticeable downregulation in upper incisor dental lamina of E11.5 *CreERT2: Rdh10*$^{flox/flox}$ mice (Fig. 4H, L) (n=4 embryos each).

Shh is another dental placode marker and is required for cell proliferation and invagination of dental epithelium during odontogenesis (Cobourne et al. 2001; Dassule et al. 2000; Li et al. 2016). The present results showed fragmented *Shh* expression in *CreERT2: Rdh10*$^{flox/flox}$ dental placode at E12.5 (Fig. 2I, M) (n=3 embryos each). Interestingly, the disturbed patterning of upper incisor dental placode was further detected by the expression of *Bmp4* in E12.5 *CreERT2: Rdh10*$^{flox/flox}$ mice (wild type=3 embryos; mutant=2 embryos). Meanwhile, we also detected noticeable reduction of *Bmp4* expression in upper incisor mesenchyme of *CreERT2: Rdh10*$^{flox/flox}$ mice (Fig. 4J, N). These results strongly suggest that RA signaling

is necessary for initiating upper incisor development. Moreover, RA is continuously required for invagination and patterning of the upper incisor by regulating *Shh* in dental epithelium and *Bmp4* in dental mesenchyme.

Inhibition of *Hh* Signaling Partially Restores Midfacial Cleft Phenotype in *CreERT2: Rdh10$^{flox/flox}$* Mice

To test our hypothesis that disturbed *Shh* signaling caused by reduced RA signaling aggravates midfacial cleft in *CreERT2: Rdh10$^{flox/flox}$* mice, we injected cyclopamine, an inhibitor of SMOOTHENED, to the pregnant dams at E11.0. Embryos were harvested at E13.0. We found 4 out of 19 *CreERT2: Rdh10$^{flox/flox}$* embryos treated with cyclopamine showed midfacial cleft. The incidence was significantly reduced compared with *CreERT2: Rdh10$^{flox/flox}$* mice (36 out of 38) when tamoxifen was administered at E7.0. Additionally, 9 out of 19 embryos showed reduced distance between the nostrils, indicating the severity and penetrance of midfacial cleft were reduced by titrated *Hh* signaling (Fig. 5A-D, appendix figure. 2). A slight decrease of ectopic nodules was also detected (Fig. 5B-C). Interestingly, fragmented upper incisors with lack of invagination of dental epithelium was still detected in the cyclopamine-treated group, while the *CreERT2: Rdh10$^{flox/flox}$* mice showed lack of incisors (Fig. 5E, G). These results indicate that misregulation of *Shh* signaling due to reduced RA signaling during embryonic craniofacial development underlies the etiology of midfacial cleft and agenesis of upper incisors.

Discussion

Rdh10 is expressed in a spatiotemporally regulated manner during craniofacial development starting at E8.0 and subsequently activates and regulates RA signaling (Sandell et al. 2012b; Sandell et al. 2007; Shannon et al. 2017). Therefore, we assessed the expression pattern of *Rdh10* and activity of RA signaling (*Rare-LacZ* reporter transgene) between wild-type and *CreERT2: Rdh10*$^{flox/flox}$ mice treated with tamoxifen at E7.0. As a result, noticeable reduction of *Rdh10* and *Rare-LacZ* expression was seen in the developing frontonasal process, which recapitulates the phenotype of *Rdh10* germline mutants showing midfacial cleft (Sandell et al. 2012b; Sandell et al. 2007). However, in contrast to the early lethality around E10.5 of *Rdh10* germline mutants, most of the *CreERT2: Rdh10*$^{flox/flox}$ mice could survive until E16.5, and thus we further identified novel phenotypes such as ectopic chondrogenesis in the derivatives of frontonasal process and upper incisor defects. In addition, as the time point of elimination of *Rdh10* was changed from E7.0 to E7.5, the severity of midfacial defects in *CreERT2: Rdh10*$^{flox/flox}$ mice changed from severe midfacial cleft with missing upper incisor to cleft lip with fragmented upper incisor, which is consistent with the differential severity of overall defects between *Rdh10*$^{-/-}$ null and *Rdh10*$^{trex/trex}$ mutants (Sandell et al. 2012b; Sandell et al. 2007; Shannon et al. 2017). Moreover, our previous report showed that eliminating *Rdh10* after E8.5 resulted in substantially milder craniofacial phenotypes (Kurosaka et al. 2017). These results suggest that fine-tuned RA signaling is strictly required during craniofacial development. Furthermore, all craniofacial phenotypes in *CreERT2: Rdh10*$^{flox/flox}$ mice were mainly detected in the frontonasal process but not in the maxillary process, indicating a critical role of *Rdh10* and RA signaling for the frontonasal process development.

Previous studies revealed that misdirected behaviors of cranial neural crest cells which populate the frontonasal process could contribute to midfacial cleft by disrupting the formation, migration, proliferation and survival of its cells (Beverdam et al. 2001; He and Soriano 2013; Ogoh et al. 2017; Teng et al. 2008). The comparable expression patterns of *Tfap2a* and *Sox9* between wild type and *CreERT2: Rdh10*$^{flox/flox}$ mice at E9.5 indicates normal formation and migration of cranial neural crest cells, which is consistent with other RA signaling-disrupted mutants (Dupé and Pellerin 2009; Schneider et al. 2001). In contrast, the significantly elevated apoptosis detected in the frontonasal mesenchyme indicates the crucial role of RA signaling for the survival of post-migratory cranial neural crest cells. *Alx* homeobox transcription factors, such as *Alx1, Alx3, Alx4*, are suggested to be associated with distinct types of human frontonasal dysplasia which exhibit midfacial cleft (El-Ruby et al. 2018; Twigg et al. 2009; Uz et al. 2010). Moreover, midfacial cleft is exhibited together with elevated apoptosis in the frontonasal mesenchyme of *Alx3/4* compound mutant mice. Additionally, *Alx1* is required for cell survival of embryonic forebrain mesenchyme (Beverdam et al. 2001; Zhao et al. 1996). Given the present results from both *in situ* hybridization and RNAseq analyses, significant reduction of *Alx1* and *Alx3* expression could be detected in the developing frontonasal process. These results suggest midfacial cleft and elevated apoptosis due to RA deficiency is at least partially mediated by reduced expression of *Alx* family genes. Since we also detected ectopic rod-like chondrogenesis in the medial nasal region of *CreERT2: Rdh10*$^{flox/flox}$ mice, we tried to gain insights into some molecules which are critical for cartilage development. Elevated *Fgf8* and *Wnt/β-catenin* signaling have been reported to induce ectopic nodules and cartilage in the chick and mouse craniofacial region (Abzhanov and Tabin 2004; Reid et al. 2011). Consistently, exaggerated expression

of *Fgf8* and β-CATENIN in the ectoderm of the medial nasal process is likely to underpin the ectopic rod-like chondrogenesis in *CreERT2: Rdh10*$^{flox/flox}$ mice.

In addition, the amount of *Shh* signaling is reported to regulate the face width and midfacial structures during craniofacial development (Brugmann et al. 2010; Muenke and Beachy 2000). Namely, antagonism or enhancement of *Shh* in the ventral forebrain or frontonasal process could correspondingly result in holoprosencephaly and hypertelorism, both of which are concurrent with various midfacial defects, including midfacial cleft and upper incisor defects (Brugmann et al. 2010; Firulli et al. 2014; Nanni et al. 2001). We have reported that RA signaling could interact with *Shh* signaling during early embryonic craniofacial development (Wang et al. 2019). Analogously, *Shh*, *Ptch1* and *Gli1*, key components of *Shh* signaling, showed persistent expansion in the ventral forebrain as well as the midfacial region of *CreERT2: Rdh10*$^{flox/flox}$ mice starting from E11.5 when tamoxifen was administered at E7.0. Interestingly, the expansion of *Shh* expression in *CreERT2: Rdh10*$^{flox/flox}$ ventral forebrain was milder when tamoxifen was administered at E7.5, and no obvious midfacial cleft was detected (Appendix figure. 3). These results indicate that an increased level of *Shh* signaling is responsible for aggravating midfacial cleft in RA-deficient mutants. Importantly, inhibiting *Hh* signaling by administering cyclopamine in *CreERT2: Rdh10*$^{flox/flox}$ mice resulted in significant amelioration of the severity and penetrance of midfacial cleft. These data demonstrate that persistent expansion of *Shh* signaling caused by reduced RA underlies the etiology of midfacial cleft.

Interestingly, *Shh* is also reported to synergize with *Fgf8* in regulating ectopic nodules and cartilage in the chick craniofacial region (Abzhanov and Tabin 2004). A slight decrease of

ectopic nodules in cyclopamine-treated mutants supported the interaction of RA, *Fgf8* and *Shh* in orchestrating craniofacial development.

Variable upper incisor defects from missing teeth to split tooth germ could be detected in *CreERT2: Rdh10*$^{flox/flox}$ mice. Interestingly, earlier (E7.0) elimination of *Rdh10* tended to exhibit missing teeth, while later (E7.5) elimination tended to show split tooth germ. These results indicate that RA signaling plays important roles for initiating and maintaining the patterning of upper incisors. Stratification and proliferation of dental epithelium are suggested to be involved in the initiation of odontogenesis (Balic 2019). We detected lack of stratification and/or invagination with decreased proliferation in dental epithelium of *CreERT2: Rdh10*$^{flox/flox}$ mice by using SOX2 and P21 as markers to indicate dental lamina and dental placode. At the same time, a series of signaling molecules which are responsible for inducing tooth development, such as *Pax9*, *Pitx2* and *Bmp4*, were down-regulated in the upper incisor region. Previous reports have suggested that downregulation of *Bmp* signaling in dental mesenchyme results in fragmented incisor placode with a disrupted pattern of *Shh* expression (Fujimori et al. 2010; Munne et al. 2010). This is the first report to indicate critical roles of RA signaling for the initiation and patterning of the upper incisors through regulating multiple genes.

Acknowledgements

To my life-coach, many thanks to Hiroshi Kurosaka and Takashi Yamashiro:

Thanks for the patience and kind help all the time on my research and life in Japan.

I am grateful to Lisa L. Sandell, Paul Trainor and Qi Wang for the valuable suggestions and opinions on my research.

A very special gratitude goes out to all down at Research Fundings for helping and providing the funding for the work.

With a special mention to Toshihiro Inubushi, Takayuki Tsujimoto, Haruka Ohara. It was fantastic to have the opportunity to work with you.

I am also grateful to Takayoshi Sakai, Susumu Tanaka and Makoto Abe with your suggestions on my thesis.

And finally, last but by no means least, also to everyone in the impact hub… it was great sharing laboratory with all of you during last four years.

Thank you very much for all your encouragement.

Citations

Abzhanov A, Tabin CJ. 2004. Shh and fgf8 act synergistically to drive cartilage outgrowth during cranial development. Dev Biol. 273(1):134-148.

Apesos J, Anigian GM. 1993. Median cleft of the lip: Its significance and surgical repair. The Cleft Palate-Craniofacial Journal. 30(1):94-96.

Balic A. 2019. Concise review: Cellular and molecular mechanisms regulation of tooth initiation. Stem Cells. 37(1):26-32.

Beverdam A, Brouwer A, Reijnen M, Korving J, Meijlink F. 2001. Severe nasal clefting and abnormal embryonic apoptosis in alx3/alx4 double mutant mice. Development. 128(20):3975-3986.

Brugmann SA, Allen NC, James AW, Mekonnen Z, Madan E, Helms JA. 2010. A primary cilia-dependent etiology for midline facial disorders. Hum Mol Genet. 19(8):1577-1592.

Cobourne MT, Hardcastle Z, Sharpe PT. 2001. Sonic hedgehog regulates epithelial proliferation and cell survival in the developing tooth germ. J Dent Res. 80(11):1974-1979.

Dassule HR, Lewis P, Bei M, Maas R, McMahon AP. 2000. Sonic hedgehog regulates growth and morphogenesis of the tooth. Development. 127(22):4775-4785.

Dupé V, Pellerin I. 2009. Retinoic acid receptors exhibit cell-autonomous functions in cranial neural crest cells. Dev Dyn. 238(10):2701-2711.

El-Ruby M, El-Din Fayez A, El-Dessouky SH, Aglan MS, Mazen I, Ismail N, Afifi HH, Eid MM, Mostafa MI, Mehrez MI et al. 2018. Identification of a novel homozygous alx4 mutation in two unrelated patients with frontonasal dysplasia type-2. Am J Med Genet A. 176(5):1190-1194.

Firulli BA, Fuchs RK, Vincentz JW, Clouthier DE, Firulli AB. 2014. Hand1 phosphoregulation within the distal arch neural crest is essential for craniofacial morphogenesis. Development. 141(15):3050-3061.

Friedl RM, Raja S, Metzler MA, Patel ND, Brittian KR, Jones SP, Sandell LL. 2019. Rdh10 function is necessary for spontaneous fetal mouth movement that facilitates palate shelf elevation. Dis Model Mech. 12(7).

Fujimori S, Novak H, Weissenböck M, Jussila M, Gonçalves A, Zeller R, Galloway J, Thesleff I, Hartmann C. 2010. Wnt/β-catenin signaling in the dental mesenchyme regulates incisor development by regulating bmp4. Dev Biol. 348(1):97-106.

He F, Soriano P. 2013. A critical role for pdgfrα signaling in medial nasal process development. PLoS Genet. 9(9):e1003851.

Kurosaka H, Iulianella A, Williams T, Trainor PA. 2014. Disrupting hedgehog and wnt signaling interactions promotes cleft lip pathogenesis. J Clin Invest. 124(4):1660-1671.

Kurosaka H, Wang Q, Sandell L, Yamashiro T, Trainor PA. 2017. Rdh10 loss-of-function and perturbed retinoid signaling underlies the etiology of choanal atresia. Hum Mol Genet. 26(7):1268-1279.

Li J, Chatzeli L, Panousopoulou E, Tucker AS, Green JB. 2016. Epithelial stratification and placode invagination are separable functions in early morphogenesis of the molar tooth. Development. 143(4):670-681.

Metzler MA, Raja S, Elliott KH, Friedl RM, Tran NQH, Brugmann SA, Larsen M, Sandell LL. 2018. Rdh10-mediated retinol metabolism and rarα-mediated retinoic acid signaling are required for submandibular salivary gland initiation. Development. 145(15).

Metzler MA, Sandell LL. 2016. Enzymatic metabolism of vitamin a in developing vertebrate embryos. Nutrients. 8(12).
Mishra S, Sabhlok S, Panda PK, Khatri I. 2015. Management of midline facial clefts. J Maxillofac Oral Surg. 14(4):883-890.
Muenke M, Beachy PA. 2000. Genetics of ventral forebrain development and holoprosencephaly. Curr Opin Genet Dev. 10(3):262-269.
Munne PM, Felszeghy S, Jussila M, Suomalainen M, Thesleff I, Jernvall J. 2010. Splitting placodes: Effects of bone morphogenetic protein and activin on the patterning and identity of mouse incisors. Evol Dev. 12(4):383-392.
Nanni L, Ming JE, Du Y, Hall RK, Aldred M, Bankier A, Muenke M. 2001. Shh mutation is associated with solitary median maxillary central incisor: A study of 13 patients and review of the literature. Am J Med Genet. 102(1):1-10.
Ogoh H, Yamagata K, Nakao T, Sandell LL, Yamamoto A, Yamashita A, Tanga N, Suzuki M, Abe T, Kitabayashi I et al. 2017. Mllt10 knockout mouse model reveals critical role of af10-dependent h3k79 methylation in midfacial development. Sci Rep. 7(1):11922.
Reid BS, Yang H, Melvin VS, Taketo MM, Williams T. 2011. Ectodermal wnt/β-catenin signaling shapes the mouse face. Dev Biol. 349(2):261-269.
Rossant J, Zirngibl R, Cado D, Shago M, Giguère V. 1991. Expression of a retinoic acid response element-hsplacz transgene defines specific domains of transcriptional activity during mouse embryogenesis. Genes Dev. 5(8):1333-1344.
Sandell LL, Kurosaka H, Trainor PA. 2012a. Whole mount nuclear fluorescent imaging: Convenient documentation of embryo morphology. Genesis. 50(11):844-850.
Sandell LL, Lynn ML, Inman KE, McDowell W, Trainor PA. 2012b. Rdh10 oxidation of vitamin a is a critical control step in synthesis of retinoic acid during mouse embryogenesis. PLoS One. 7(2):e30698.
Sandell LL, Sanderson BW, Moiseyev G, Johnson T, Mushegian A, Young K, Rey JP, Ma JX, Staehling-Hampton K, Trainor PA. 2007. Rdh10 is essential for synthesis of embryonic retinoic acid and is required for limb, craniofacial, and organ development. Genes Dev. 21(9):1113-1124.
Schneider RA, Hu D, Rubenstein JL, Maden M, Helms JA. 2001. Local retinoid signaling coordinates forebrain and facial morphogenesis by maintaining fgf8 and shh. Development. 128(14):2755-2767.
Shannon SR, Moise AR, Trainor PA. 2017. New insights and changing paradigms in the regulation of vitamin a metabolism in development. Wiley Interdiscip Rev Dev Biol. 6(3).
Sun Z, Yu W, Sanz Navarro M, Sweat M, Eliason S, Sharp T, Liu H, Seidel K, Zhang L, Moreno M et al. 2016. Sox2 and lef-1 interact with pitx2 to regulate incisor development and stem cell renewal. Development. 143(22):4115-4126.
Teng L, Mundell NA, Frist AY, Wang Q, Labosky PA. 2008. Requirement for foxd3 in the maintenance of neural crest progenitors. Development. 135(9):1615-1624.
Thesleff I. 2003. Epithelial-mesenchymal signalling regulating tooth morphogenesis. J Cell Sci. 116(Pt 9):1647-1648.
Twigg SR, Versnel SL, Nürnberg G, Lees MM, Bhat M, Hammond P, Hennekam RC, Hoogeboom AJ, Hurst JA, Johnson D et al. 2009. Frontorhiny, a distinctive presentation of frontonasal dysplasia caused by recessive mutations in the alx3 homeobox gene. Am J Hum Genet. 84(5):698-705.

Uz E, Alanay Y, Aktas D, Vargel I, Gucer S, Tuncbilek G, von Eggeling F, Yilmaz E, Deren O, Posorski N et al. 2010. Disruption of alx1 causes extreme microphthalmia and severe facial clefting: Expanding the spectrum of autosomal-recessive alx-related frontonasal dysplasia. Am J Hum Genet. 86(5):789-796.

Wang Q, Kurosaka H, Kikuchi M, Nakaya A, Trainor PA, Yamashiro T. 2019. Perturbed development of cranial neural crest cells in association with reduced sonic hedgehog signaling underlies the pathogenesis of retinoic-acid-induced cleft palate. Dis Model Mech. 12(10).

Zhang L, Yuan G, Liu H, Lin H, Wan C, Chen Z. 2012. Expression pattern of sox2 during mouse tooth development. Gene Expr Patterns. 12(7-8):273-281.

Zhao Q, Behringer RR, de Crombrugghe B. 1996. Prenatal folic acid treatment suppresses acrania and meroanencephaly in mice mutant for the cart1 homeobox gene. Nat Genet. 13(3):275-283.

Figures

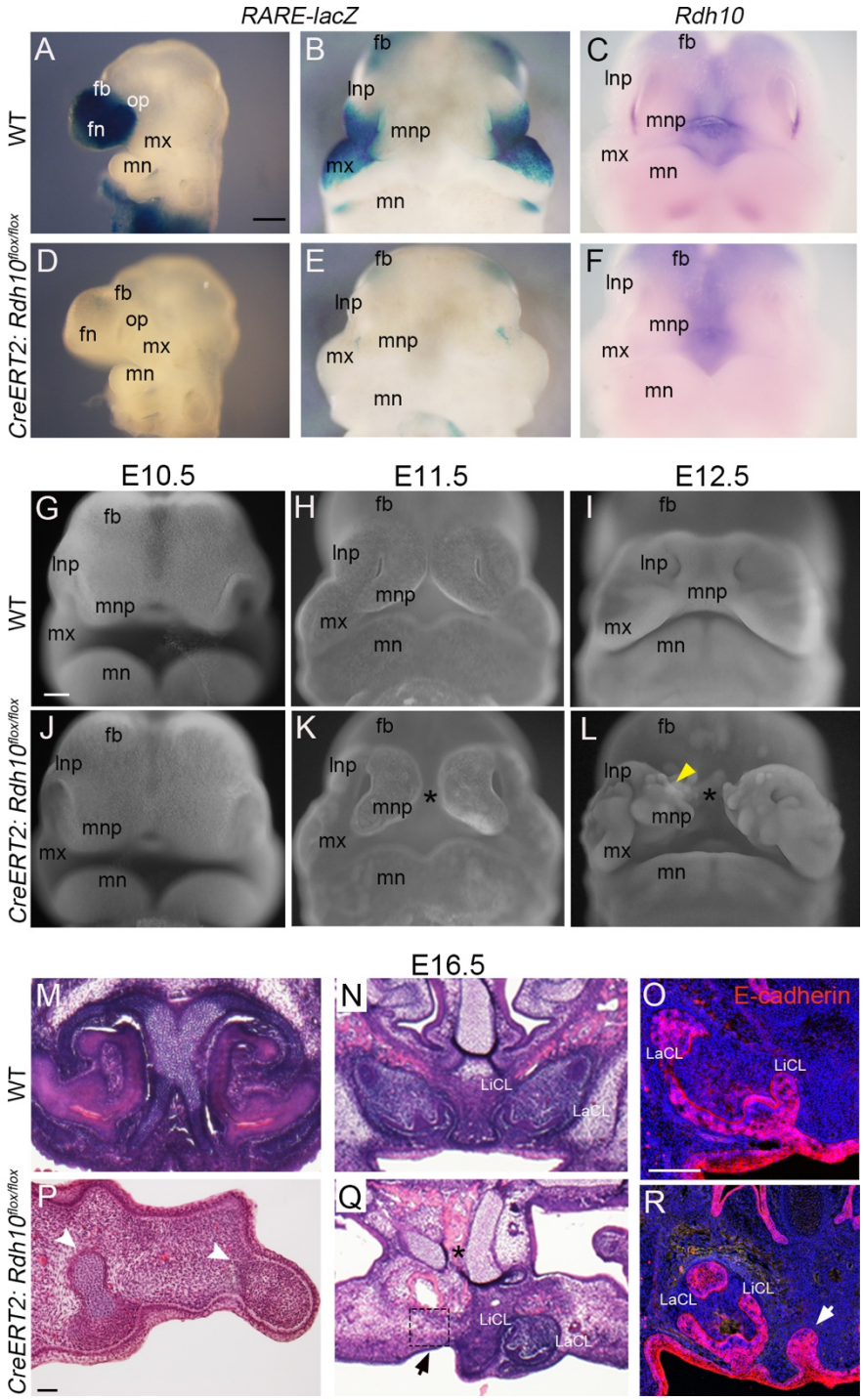

Figure 1. Facial and dental phenotypes of *CreERT2:Rdh10*$^{flox/flox}$ mutant mice. **(A-F)** Comparison of *Rdh10* and *RARE-lacZ* expression between wild-type and

CreERT2:Rdh10$^{flox/flox}$ mice. Lateral view of *RARE-lacZ* expression in E9.5 wild-type (A) and *CreERT2: Rdh10*$^{flox/flox}$ mice (D). Frontal view of *RARE-lacZ* expression in E10.5 wild-type (B) and *CreERT2: Rdh10*$^{flox/flox}$ mice (E). Frontal view of *Rdh10* mRNA expression in E10.5 wild-type (C) and *CreERT2: Rdh10*$^{flox/flox}$ mice (F). Scale bar in A, 200 μm. **(G-L)** Frontal view of whole-mount nuclear fluorescent imaging between wild-type and *CreERT2: Rdh10*$^{flox/flox}$ mice. E10.5(G, J), E11.5(H, K), E12.5(I, L) whole-mount nuclear fluorescent imaging of wild-type (G-I) and *CreERT2: Rdh10*$^{flox/flox}$ mice (J-L). The yellow arrowhead in L indicates ectopic nodules on the face. Asterisks in K and L indicate the midfacial cleft. Scale bar in G, 200 μm. (M-R**)** Frontal histological sections of E16.5 heads of wild-type (M-O) and *CreERT2: Rdh10*$^{flox/flox}$ mice (P-R). Hematoxylin and eosin stained paraffin sections of the ectopic nodules (M, P) and the upper incisors (N, Q). The white arrowheads in P indicate abnormal mesenchyme condensation and chondrogenesis on the face. Asterisk in Q indicates split nasal septum. The black arrow in Q indicates missing upper incisor tooth germ. Scale bar in P, 50 μm. (O, R) E-Cadherin was stained in red. The white arrow in R indicates split upper incisor tooth germ. Tamoxifen was administered at E7.0 in (A-L) and E7.5 in (M-R). Scale bar in O, 100 μm. fb, forebrain; fn, frontonasal process; lnp, lateral nasal process; LaCL, labial cervical loop; LiCL, lingual cervical loop; mnp, medial nasal process; mx, maxillary process; mn, mandible process; op, optic.

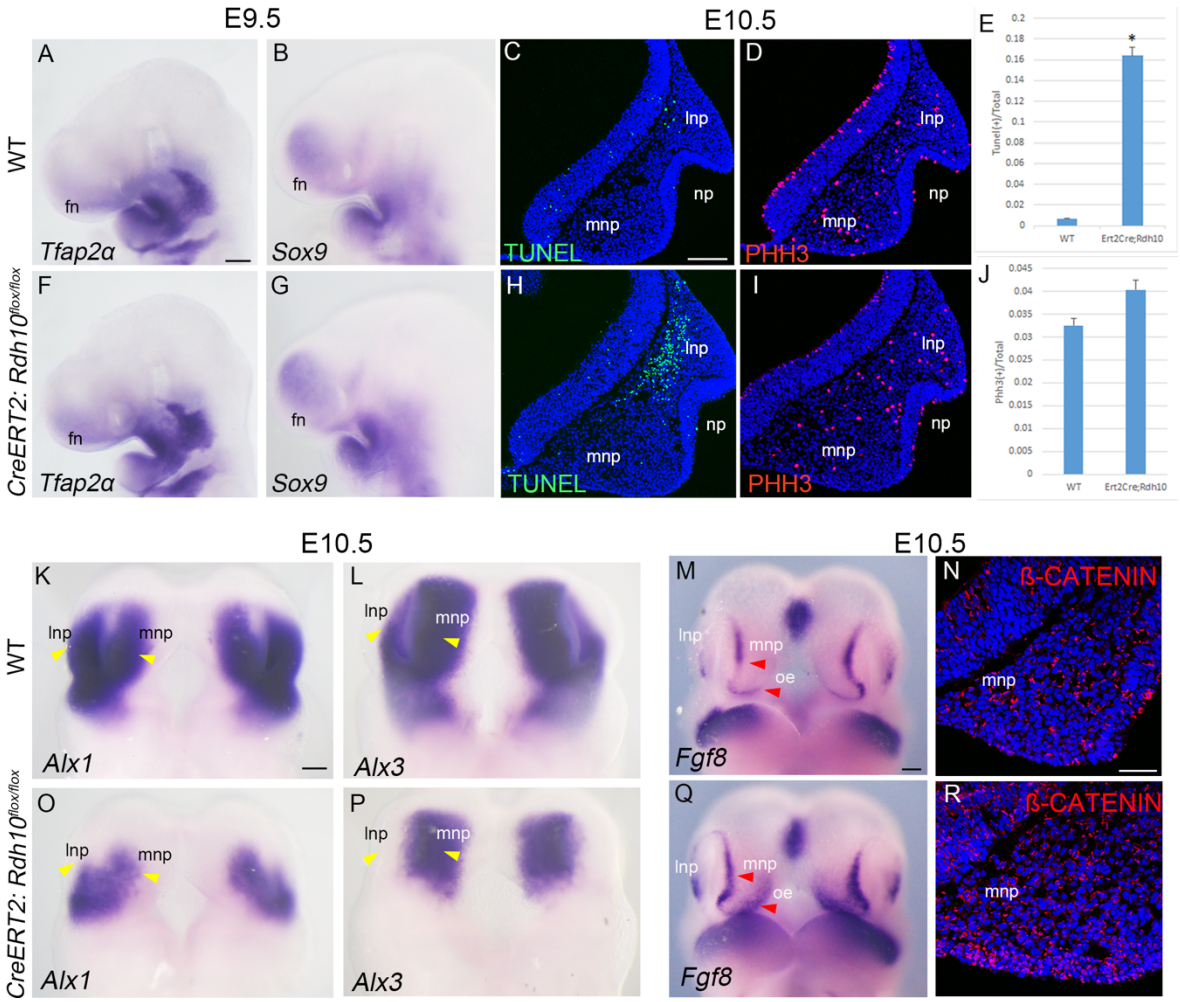

Figure 2. Analysis of cranial neural crest cells' behavior and expression of molecular markers in developing facial processes. **(A-J)** Migration, apoptosis and proliferation of cranial neural crest cells in wild-type and *CreERT2: Rdh10*$^{flox/flox}$ mice. Lateral view of *Tfap2a* (A, F) and *Sox9* (B, G) expression in E9.5 wild-type (A, B) and *CreERT2: Rdh10*$^{flox/flox}$ mice (F, G). Frontal sections of E10.5 heads from wild-type (C, D) and *CreERT2: Rdh10*$^{flox/flox}$ mice (H, I). TUNEL staining is shown in green (C, H) and phospho-Histone-H3 (PHH3) is in red (D, I). Statistical analysis of the ratio of TUNEL-positive cells (TUNEL+) (E) and PHH3-positive cells (PHH3+) (J) within the mesenchymal cells in frontonasal process. Asterisk, P<0.05. Scale bar in A, 200 µm; C, 100 µm. **(K-R)** Assessment of certain gene expression profiles in wild-type and *CreERT2:Rdh10*$^{flox/flox}$ frontonasal process. Whole-mount *in situ* hybridization of *Alx1* (K, O), *Alx3* (L, P). The yellow arrowheads in K, L, O, and P indicate the reduction of *Alx1* and *Alx3* expression

levels. Frontal view of *Fgf8* expression in E10.5 wild-type (M) and *CreERT2: Rdh10*$^{flox/flox}$ mice (Q). The red arrowheads indicate the elevation of *Fgf8* expression in *CreERT2: Rdh10*$^{flox/flox}$ mice. β-CATENIN localization is shown in red by immunohistochemistry in frontal sections of medial nasal process in E10.5 wild-type (N) and *CreERT2:Rdh10*$^{flox/flox}$ mice (R). Tamoxifen was administered at E7.0 in (A-R). Scale bar in K and M, 200 μm; N, 50 μm. fn, frontonasal process; lnp, lateral nasal process; mnp, medial nasal process; np, nasal pit; oe, oral ectoderm.

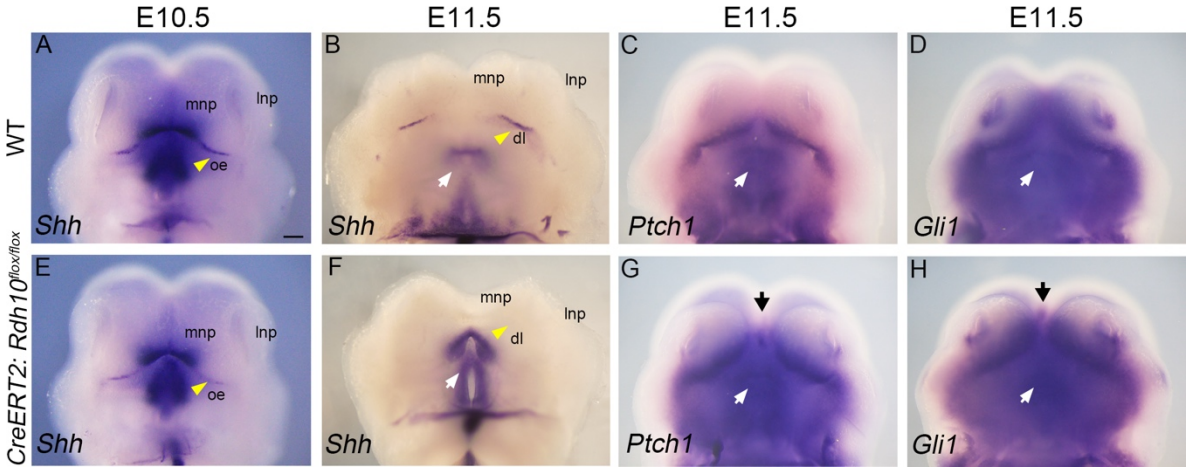

Figure 3. Disrupted *Shh* signaling in *CreERT2:Rdh10*$^{flox/flox}$ mice. **(A-H)** Whole-mount *in situ* hybridization of *Shh*, *Ptch1* and *Gli1* compared between wild-type (A-D) and *CreERT2:Rdh10*$^{flox/flox}$ mice (E-H). Ventral view of *Shh* expression in E10.5 (A, E) and E11.5 (B, F) embryos. The yellow arrowheads in A, B, E, and F indicate reduced *Shh* expression levels in oral ectoderm and dental lamina of *CreERT2:Rdh10*$^{flox/flox}$ mice. Ventral view of *Ptch1* (C, G) and *Gli1* (D, H) expression in E11.5 embryos. The white arrows in B-D and F-H indicate persistent expression of *Shh*, *Ptch1* and *Gli1* expression in the ventral forebrain of *CreERT2:Rdh10*$^{flox/flox}$ mice. The black arrows in G and H indicate ectopic *Ptch1* and *Gli1* expression in midline of the face of *CreERT2:Rdh10*$^{flox/flox}$ mice. Tamoxifen was administered at E7.0 in (A-H). Scale bar in A, 200 μm. dl, dental lamina; lnp, lateral nasal process; mnp, medial nasal process; oe, oral ectoderm.

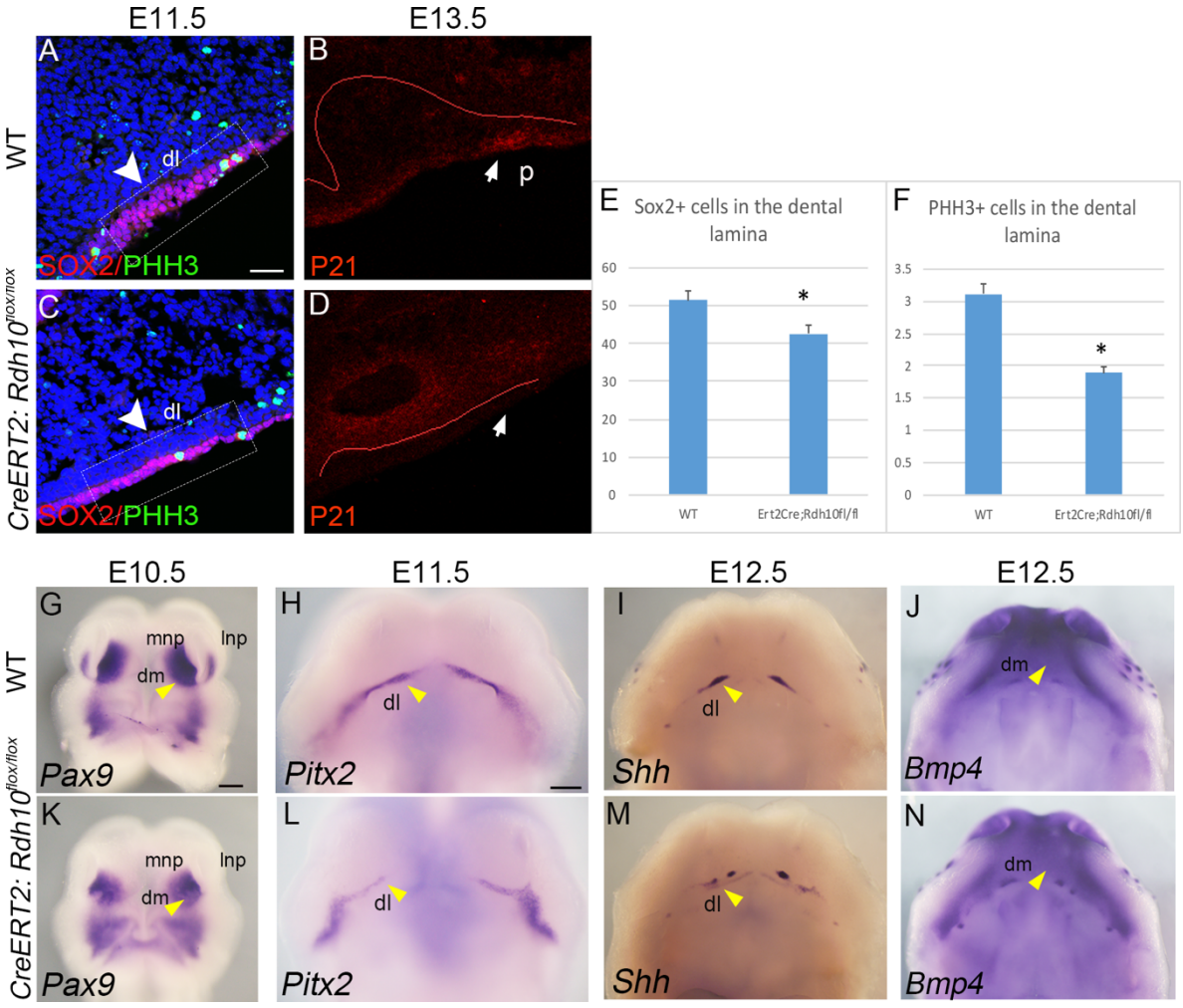

Figure 4. Cytological and molecular assessment of incisor development. **(A-F)** Frontal sections of E11.5 (A, C) and E13.5 (B, D) upper incisors from wild type (A-B) and *CreERT2: Rdh10*$^{flox/flox}$ mice (C-D). *Sox2* is shown in red to indicate the dental lamina and phospho-Histone-H3 (PHH3) is shown in green (A, C). The white arrowheads in A and C indicate loss of epithelial stratification in the dental lamina in E11.5 *CreERT2: Rdh10*$^{flox/flox}$ mice. P21 is shown in red to indicate the dental placode (B, D). The white arrows in B and D indicate the lack of dental placode in E13.5 *CreERT2: Rdh10*$^{flox/flox}$ mice. Statistical

analysis showed significantly reduced number of *Sox2*- and PHH3-positive cells in *CreERT2: Rdh10*$^{flox/flox}$ mice dental lamina (E and F). Asterisk, *P*<0.05. Scale bar in A, 25 μm. **(G-N)** Whole-mount *in situ* hybridization of *Pax9* (G, K), *Pitx2* (H, L), *Shh* (I, M) and *Bmp4* (J, N) comparison between wild-type (G-H) and *CreERT2: Rdh10*$^{flox/flox}$ mice (K-N). The yellow arrowheads in G-N indicate the reduced expression of indicated genes in *CreERT2: Rdh10*$^{flox/flox}$ mice. Tamoxifen was administered at E7.0 in (A-H, K, L) and E7.5 in (I, J, M, N). Scale bar in G, 200 μm. dl, dental lamina; dm, dental mesenchyme; lnp, lateral nasal process; mnp, medial nasal process; p, dental placode.

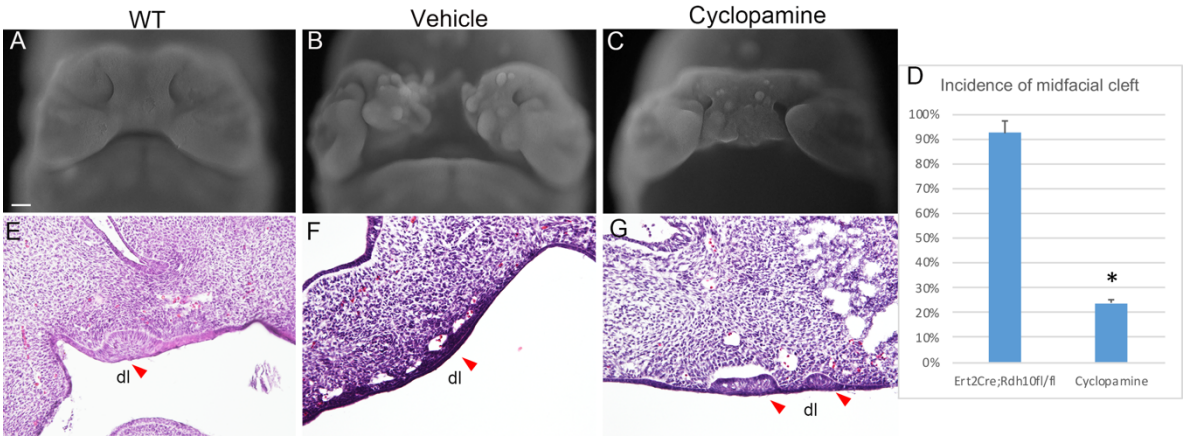

Figure 5. Modification of midfacial cleft phenotype via inhibition of *Hh* signaling. **(A-C)** Whole-mount nuclear fluorescent imaging of wild type (A), *CreERT2: Rdh10*$^{flox/flox}$ mice without cyclopamine treatment (B) and cyclopamine-treated *CreERT2: Rdh10*$^{flox/flox}$ mice (C). Frontal view of E13.0 embryos (A-C). **(D)** The incidence of midfacial cleft in cyclopamine-treated *CreERT2: Rdh10*$^{flox/flox}$ mice showed significant reduction compared to the non-treated group (D). Asterisk, *P*<0.05. **(E-G)** Hematoxylin and eosin staining of frontal sections of the upper face of the mice in (A-C). The red arrowheads in E-G indicate the dental lamina. Scale bar in A and E, 200 μm. dl, dental lamina.

Appendix Figures

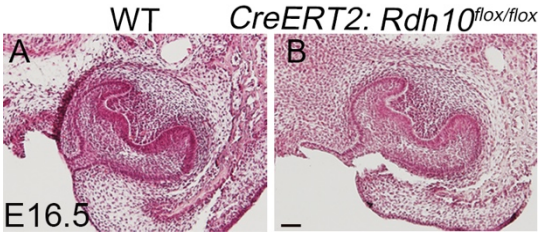

Appendix Figure 1. Morphological analysis of the upper molars. **(A-B)** Hematoxylin and eosin stained frontal sections of the upper molars in wild type (A) and *CreERT2: Rdh10*$^{flox/flox}$ mice (B). Scale bar in B, 50 μm.

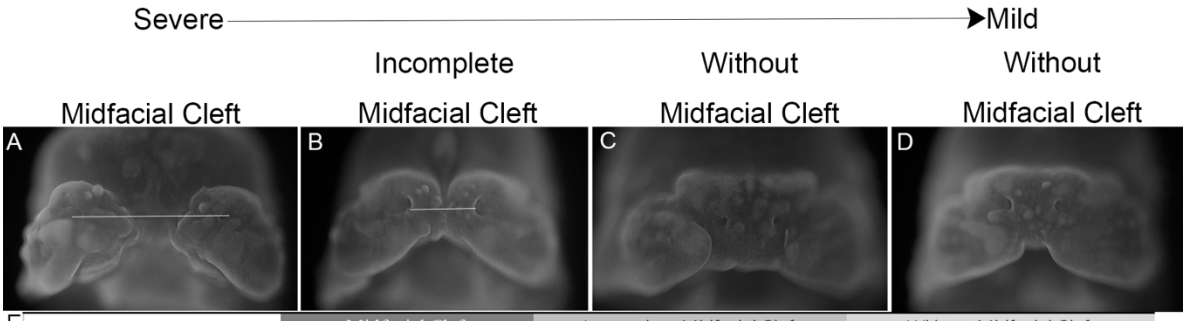

E

	Midfacial Cleft	Incomplete Midfacial Cleft	Without Midfacial Cleft
CreERT2: Rdh10flox/flox Cyclopamine (-)	36 out of 38 embryos	0	2 out of 38 embryos
CreERT2: Rdh10flox/flox Cyclopamine (+)	4 out of 19 embryos	2 out of 19 embryos	7 out of 19 embryos

Appendix Figure 2. Phenotypes of cyclopamine-treated mutants. **(A-D)** Whole-mount nuclear fluorescent imaging of cyclopamine-treated *CreERT2: Rdh10*$^{flox/flox}$ mice. **(E)** Phenotypic variation of *CreERT2: Rdh10*$^{flox/flox}$ embryos with or without cyclopamine treatment. The white bars in A and B indicate the distance between the nostrils.

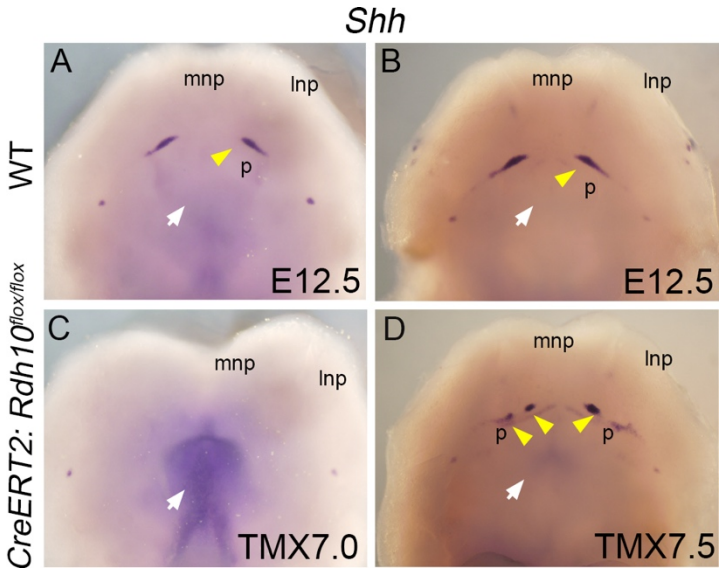

Appendix Figure 3. Differentially disrupted pattern of *Shh* expression with different time points of tamoxifen treatment. **(A-D)** Whole-mount in situ hybridization of *Shh* in wild-type (A-B) and *CreERT2: Rdh10*$^{flox/flox}$ mice (C-D). Ventral view of *Shh* expression with tamoxifen treatment at E7.0 (A, C) and E7.5 (B, D). The white arrows in A-D indicate persistent expansion of *Shh* in the ventral forebrain. The yellow arrowheads in A, B, and D indicate *Shh* marked dental placode. p, dental placode.